Check for updates

◆ ANNUAL ISSUE

EARLY CAREER SCHOLARS IN MATERIALS SCIENCE 2023

# Review on magnetocaloric high-entropy alloys: Design and analysis methods

Jia Yan Law[1,a] (iD), **Victorino Franco**[1] (iD)
[1] *Department of Condensed Matter Physics, ICMS-CSIC, University of Seville, P.O. Box 1065, 41080 Seville, Spain*
[a] Address all correspondence to this author. e-mail: jylaw@us.es

The search for high-performance functional alloys with improved service life and reliability entails the optimization of their mechanical properties. Recently, the high-entropy alloy (HEA) design concept has found new alloys with excellent mechanical properties. It utilizes multiprincipal elements to yield high configurational entropy of mixing, entailing a large compositional freedom with wide window of opportunities for property exploration. Their functional properties are usually modest when compared to conventional materials. The discovery of HEAs with optimal combination of mechanical and functional properties would be a leap forward in the reliability of functional devices. This review article focuses on magnetocaloric HEAs, the design approaches, and the appropriate analysis methods for their performance. We will highlight the efficient strategic search within the vast HEA space, which has been instrumental for significantly enhancing MCE performance, closing the pre-existing gap between magnetocaloric HEAs and high-performance conventional magnetocaloric materials. Outlook for future directions will also be included.
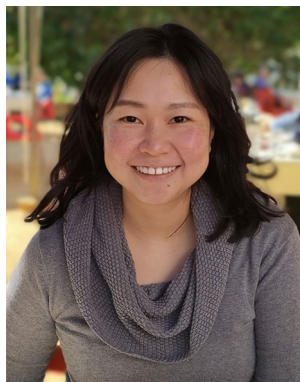
Jia Yan Law

Jia Yan Law has been awarded in 2022 an Emergia Fellowship from the Regional Government of Andalucía (Spain) to focus on the study of functional high-entropy alloys. In addition to this, she has been awarded grants from Plan Propio de Investigación from University of Seville in 2021 and 2022 and is currently the co-PI with Prof. V. Franco (University of Seville) of a US Air Force Office of Scientific Research Grant in which she leads the part on HEA research. Previously, she held postdoctoral research positions at IMDEA Nanoscience (Spain), Chalmers University of Technology (Sweden) and her alma mater, Nanyang Technological University (Singapore). She graduated with B.Eng (Materials Engineering, Hons.) in 2007 and Ph.D. (Materials Science and Engineering) in 2012, both from Nanyang Technological University. Highlights of her work involve demonstration device of transient cooling by the magnetocaloric effect, the criterion to quantitatively identify first-order thermomagnetic phase transitions and the large MCE improvement found for HEAs. She has received awards for her work excellence, which includes University of Seville Award for Research Work of Special Relevance 2020, Best Paper of the Year 2018 Award, Science Paper Award of the month (from 2018 – 2021), IEEE Magnetic Society Summer School – Singapore Chapter Best Poster Award 2011. Jia Yan has been invited to give lectures and keynote presentations at international and national conferences. She also serves as the Special Events Chair of 67th Annual Conference on Magnetism and Magnetic Materials (MMM 2022) and Program co-chair of IEEE International Conference on Nanotechnology 2024 (IEEE Nano 2024). She was Secretary-Treasurer of the 23rd Soft Magnetic Materials Conference and Editor for the 25th Soft Magnetic Materials Conference, and for the 2020 and 2022 Magnetism and Magnetic Materials Conferences. In 2022, she has been appointed Editor for IEEE Magnetics Society Newsletter.

Introduction

The motivation for studying HEA for magnetocalorics

Data statistics consolidated by Enerdata © show a long-term trend of increasing electricity consumption [1]. This prompts for energy efficiency concerns in order to maintain sustainable living. The magnetocaloric effect (MCE), which describes the reversible temperature change of a magnetic material when subjected to an adiabatically varying magnetic field, forms the basis of magnetic refrigeration. Utilizing solid magnetic material as the regenerator bed, this cooling technology does not rely on ozone-depleting or hazardous gaseous refrigerants used in conventional vapor-compression refrigerators and at the same time offers a noiseless system (omitting the compressor). In addition, with an attractive energy efficiency in magnetic refrigeration (doubling that of conventional refrigerators), magnetocalorics would be very useful for specialty applications, such as the refrigeration in space or submarine settings where noiseless, space-saving and avoidance of compressed gases would be crucial. Additionally, it could address some of the global energy issues we face today in a more environmental-friendly way. However, to make this promise a reality, the ongoing search of appropriate magnetocaloric material with optimized performance including mechanical stability is crucial.

A new revolutionary material design concept has found new alloys with excellent mechanical properties, corrosion and radiation resistance [2]. It is widely known as the High Entropy Alloy (HEA) design concept and it is the current go-to technique when it comes to designing materials for structural / defense-related applications. The approach utilizes a combination of multiprincipal elements in large proportions to yield high configurational entropy of mixing (ΔS_{mix}) values. HEAs are originally sought for within single-phase solid solution metallic alloys but today the focus has expanded to multiphases and intermetallics / ceramics. This entails a large compositional freedom with wide window of opportunities for property exploration. Hence, applying the HEA design concept for developing magnetocaloric materials would create new combined capabilities of high performance and improved material service life.

Current state-of-the-art of high-entropy alloys in the field of magnetocalorics

High-entropy alloys (HEAs) have received a global interest since their discovery with outstanding mechanical properties, being a rapidly growing field of research. The number of their publications has tremendously surged: an increase of 32% in annual publications for 2021 vs. 2020; Web of Science (WoS) bibliographic search (up to May 2022) already shows a record
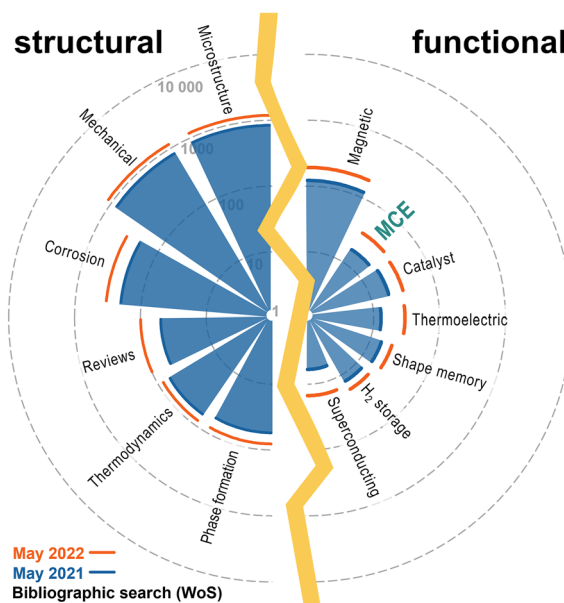

Figure 1: The number of HEA research articles and their different focus (mechanical properties, microstructure, etc.) presented in log scale. Bibliographic search was restricted to article titles containing "high-entropy*" with the focus labels (surveyed in WoS up to May 2022).

of 732 publications for 2022, which is expected to increase by the year's end. However, these endeavors are mainly focused on mechanical properties and structural applications while functional reports are scarce (5% out of the total number of publications are for functional high-entropy materials). As an example, we present the cumulative number of HEA research articles as shown in Fig. 1 and their different focus topics for 2021 (blue shaded regions) and 2022 (orange solid lines). The WoS survey shows that the structural reports (on the left of Fig. 1) clearly surpass those of the functional endeavors (on the right of Fig. 1), being magnetic and MCE of HEAs receiving most attention among the functional properties.

Fundamentals

The magnetocaloric effect

The magnetocaloric effect (MCE) refers to the reversible temperature change of a magnetic material when adiabatically magnetized or demagnetized. During this process, the magnetic field manipulates the degrees of freedom of the magnetic sub-lattice including their coupling to the degrees of freedom associated with the structure. Hence, MCE can be indirectly determined from the isothermal entropy change correlated with magnetization from the following equation as derived from the Maxwell relation:
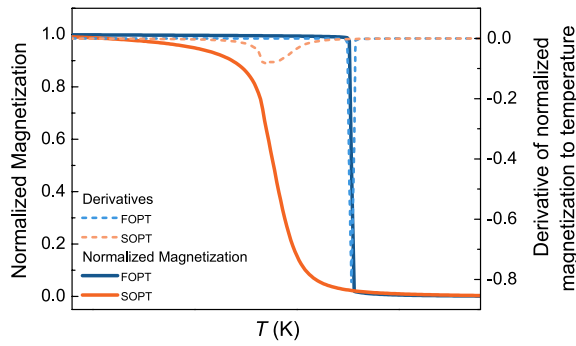
Figure 2: Left y-axis: normalized magnetization of FOPT (blue) and SOPT (orange) magnetocaloric material. Right y-axis: Derivatives of magnetization vs temperature (dashed lines) which are directly related to $\Delta S_{isothermal}$ according to Eq. 1. Hence, the peak values of MCE lie in the vicinity of the transition temperatures of the materials where the change of magnetization with respect to temperature plays a crucial role in MCE magnitude.

$$\Delta S_{isothermal} = \mu_0 \int_{(H_{initial})}^{(H_{final})} \frac{\partial M}{\partial T} dH, \tag{1}$$

where $\Delta S_{isothermal}$ refers to the isothermal entropy change, H is the magnetic field, M represents magnetization and T is temperature. Therefore, for materials exhibiting an abrupt change of magnetization with temperature influenced by magnetic field a considerable MCE will be observed. In other words, MCE would peak near the transition temperature of the magnetic material since $\Delta S_{isothermal}$ is directly related to $\partial M/\partial T$ as depicted in Fig. 2.

In general, magnetocaloric materials are classified according to their order of phase transitions, namely first-order phase transition (FOPT) and second-order (or higher order) phase transition (SOPT). It has been reported that Eq. 1 can be directly applied to materials that undergo SOPT while discontinuous measurement protocols are essential for FOPT materials in order to use the same equation for determining MCE without the influence of prior history of the sample during each set of measurements. Ref. [3] contains details of the various discontinuous measurement protocols for performing magnetization measurements to determine for the MCE appropriate for both types of magnetocaloric materials. For reviews on magnetocalorics, one can refer to recent comprehensive reports on materials [4–6] and devices [7].

HEA

Rather than employing one or two main constituents in the traditional alloy development method, HEAs adopt a different design concept that blends multiple principal elements in large concentrations without any base element. In that way, they form multi-principal elements alloys of high values of configurational entropy

of mixing (ΔS_{mix}), focusing on the central regions of multicomponent phase diagrams as illustrated in the ΔS_{mix} contour plot in Fig. 3. For simplicity, a ternary alloy system is used for illustration, where it can be noticed that ΔS_{mix} increases as the composition approaches the central equiatomic region, arriving at a maximum value. HEAs were originally defined comprising of five or more principal elements in equiatomic compositions being single-phase random solid solution metallic alloys. Today, the HEA design has expanded from equiatomic to non-equiatomic compositions, enabling a greater compositional space than that of the traditional alloying method and thus permits new (and more) viable element combinations and interesting properties to be discovered. Hence, the scope of HEA research now also includes materials of four principal elements, intermetallic and ceramic compounds, including microstructures of any number and type of phases [8]. Thus, alternative names to HEAs can be found for embracing this broader research scope: complex concentrated alloys (CCAs) and high-entropy materials (HEMs). In general, there are two widely accepted ways of defining HEAs [8, 9]:

Composition-based definition

In early reports, HEAs had been defined with five or more principal elements in equiatomic compositions [10]. Today, with more knowledge about this new class of materials from their growing works, this restricted definition is expanded to a compositional definition: alloys that include multiple principal elements with concentration of each element being 5 to 35 atomic percent (at.%), which could also contain minor elements for property tuning purposes [8].

This composition-based definition for HEAs further expands the compositional space from equiatomic to non-equiatomic regions and is not restricted to requirement of single-phase solid solutions.

Entropy-based definition

For this definition, the equation to calculate for ΔS_{mix} is

$$\Delta S_{mix} = R \sum x_i \ln x_i \tag{2}$$

where R is the gas constant and x_i is the mole fraction of the ith element. The threshold for HEA design utilizes $\Delta S_{mix} \geq 1.5\,R$ though other definitions or interpretations (i.e., 1.61 R) could be found in the literature. As an example, a quinary alloy formula of 5–35 at.% will yield $\Delta S_{mix} = 1.36$ R (35% A, 35% B, 20% C, 5% D and 5% E) while the ΔS_{mix} value of 1.61 R is the maximum attainable for a quinary HEA in equiatomic compositions. This case would be considered a HEA by the composition-based definition but not by the entropy-based one. To find a compromise between both definitions, it is currently accepted that $\Delta S_{mix} \geq 1.5$ R is the threshold for being considering a HEA. There have been

several modifications and compromises between these definitions, being the most general the compositional one. For further details, the reader is referred to Ref. [8].

Typical MCE-HEA design strategies

The search for magnetocaloric HEAs was traditionally centered on the equiatomic compositional design and usually comprised of fully rare-earth (RE) elements or a mixture of RE and transition metal (TM) elements. For the former, they yield zero enthalpy of mixing values and small atomic radii difference, resulting in crystalline microstructures. On the other hand, RE-TM HEAs yield negative enthalpy of mixing values and large atomic radii difference, which frustrates crystallization and form high-entropy bulk metallic glasses (HE-BMGs). As microstructures could be further manipulated through thermal processing, there are more works on magnetocaloric HE-BMGs than RE-HEAs, with ref. [11] covering a comprehensive discussion in bringing together how the different reports (or compositions) are interlinked to one another. In addition to compositional search or effects of processing, many of the early results focus on the tunability of the transition temperatures and the exploitation of distributed exchange considering the d-orbital overlap [12–15]. Recently, magnetocaloric HEA reports evolve to the exploration of the non-equiatomic region, finding MCE that surpasses the previous limitations of RE-HEAs and RE-free HEAs. In the following sections, we will highlight the methods by which magnetocaloric HEAs are designed, their limitations, as well
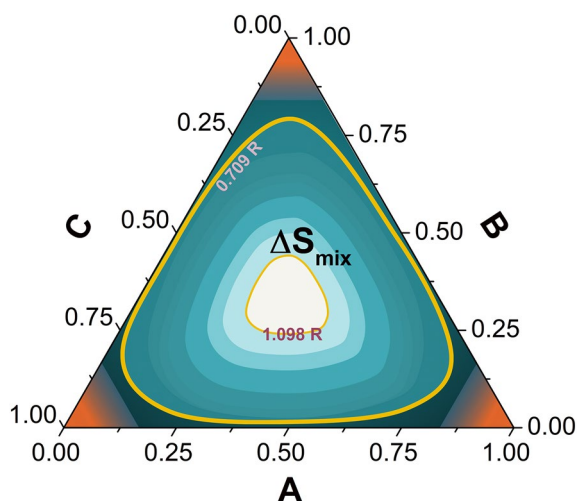

Figure 3: Contour plot of ΔS_{mix} for a model ternary alloy. Conventional alloys based on 1 or 2 constituents are found at the corners and edges. As the alloy compositions modify toward large proportion of each element, ΔS_{mix} values are also observed to increase (as we move toward the center of the plot). The largest ΔS_{mix} is found at the center of the plot, where the elements are in equiatomic compositions.
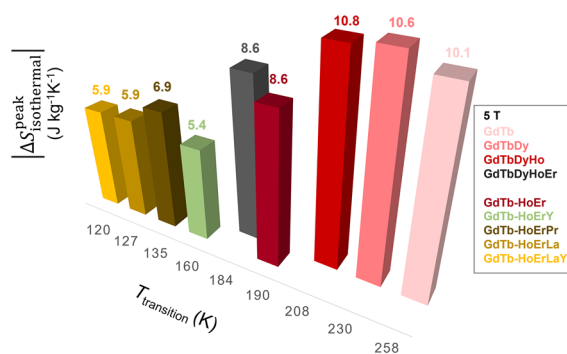

Figure 4: The magnetocaloric effect depends on the nature of the selected element when designing HEAs by increasing number of principal elements. Data taken from refs. [17–19].

as how to approach the design in the non-equiatomic regions in an efficient manner.

Increasing number of principal elements

The most common approach for designing magnetocaloric HEAs is to increase the number of principal elements in equiatomic proportions toward the HEA definition. This was firstly reported by Yuan et al. [16]. They found that the peak isothermal entropy change, $\left|\Delta S_{isothermal}^{peak}\right|$, values (and transition temperatures, $T_{transition}$) increase as they tune from ternary TbHoEr → quaternary GdTbHoEr → quinary GdTbDyHoEr. Following this approach, other magnetocaloric rare-earth (RE) HEA with increasing ΔS_{mix} values were reported, with their data being summarized in Fig. 4. As presented in the figure legend, the works can be classified into two series: Dy-containing and Dy-free. For the former [17], though the $\left|\Delta S_{isothermal}^{peak}\right|$ values (including their $T_{transition}$) decrease from -10 ± 1 to 8.6 J kg^{-1} K^{-1} (for a field of 5 T) when increasing the number of principal elements to GdTbDyHoEr, such a MCE magnitude could still be considered a relatively good magnetocaloric material. On the other hand, the trend of Dy-free series is less straightforward. Overall, the MCE decreases when tuning from quaternary to quinary or senary HEA in equiatomic compositions. Among the quinary and senary HEAs, the addition of magnetic Pr to form GdTbHoErPr enables the highest $\left|\Delta S_{isothermal}^{peak}\right|$ value, unlike the additions of non-magnetic Y and La. Furthermore, the comparison of these works (as shown in Fig. 4) reveals that the design strategy by increasing ΔS_{mix} of magnetocaloric HEA is highly dependent on the nature of the selected elements (in this case, the number of $4f$ electrons of the RE element) for the alloy composition including their proportions (though the reported studies focus only on equiatomic amounts). In other words, it is not very likely to experimentally find remarkable MCE in these novel compositions in an efficient manner without an extensive trial and error approach.
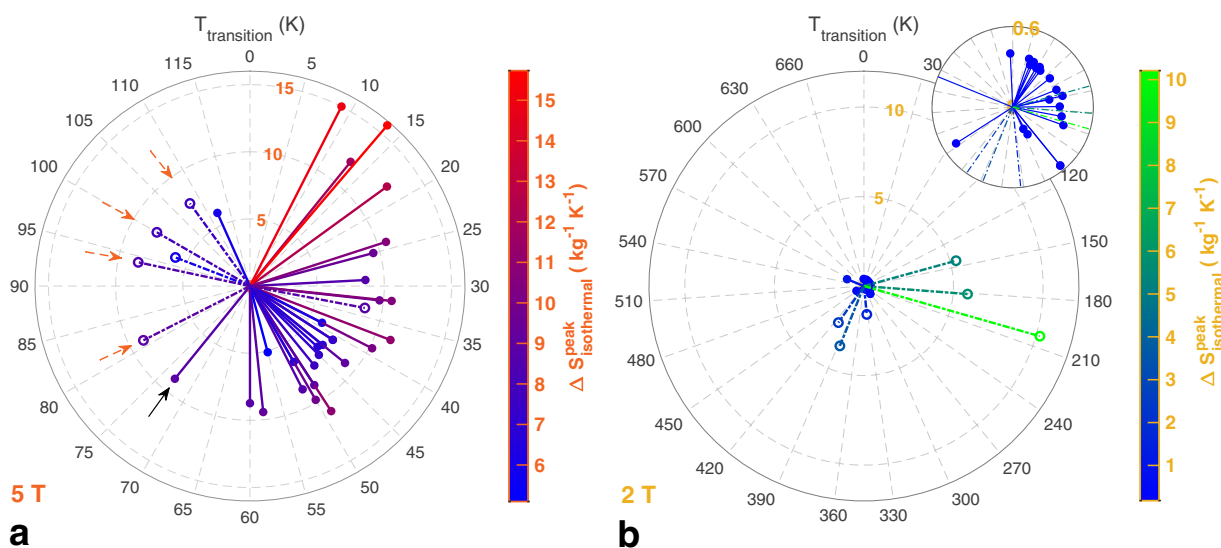
Figure 5: Magnetocaloric performance of HEAs for (a) RE-amorphous (5 T) and RE-free HEA (2 T): equiatomic (solid symbols) versus non-equiatomic (open circles). Arrows in (a) indicate the evolution from equiatomic to non-equiatomic (see text). Inset in (b): A magnified subplot for equiatomic RE-HEAs with smaller scale limits.

Extending toward the non-equiatomic high-entropy regions

HEAs started with an initial design concept of a single-phase solid solution comprising of more than five major elements. Very commonly, these multicomponent alloys present more than one phase when advanced microscopic investigations are performed, which drove many efforts in the direction of understanding or predicting the phase formation in this vast compositional space. As more HEA studies enable better understanding about this new class of materials, their earlier limitations to the abovementioned definitions have evolved to encompassing non-equiatomic multiphase alloys, including intermetallic and ceramics, forming the second-generation HEAs [2]. With the HEA concept evolution, it enables more novel materials to be designed and fabricated as well as to meet specific needs of the applications, which are very crucial in functional aspects. Many structural second-generation HEAs are found with remarkable properties that are formerly not found in first-generation HEAs and conventional alloys [20].

For magnetocalorics, the second-generation HEAs of non-equiatomic compositions has overcome the previous limitations of equiatomic magnetocaloric HEAs. For the RE-containing amorphous HEAs as presented in Fig. 5a, the equiatomic compositions (see the solid symbols) show transition temperatures ($T_{transition}$) that tend to cluster at low temperatures (< 75 K) though they can show significant MCE. Taking the RE-containing amorphous HEA with the highest $T_{transition}$ (i.e., 73 K) whose composition is GdTbCoAl (marked by black arrow), its non-equiatomic $Gd_{36}Tb_{20}Co_{20}Al_{24}$ counterpart attains $T_{transition} = 81$ K, which shows an increase of 11% [21]. With

minor Fe additions to $Gd_{36}Tb_{20}Co_{20}Al_{24}$, $T_{transition}$ as high as 108 K is found, overcoming the previous low temperature limit of RE-containing amorphous HEAs. These compositions are marked by orange arrows in Fig. 5a. Unlike the RE-containing HEAs, magnetocaloric RE-free HEAs (see Fig. 5b) are not limited to low temperature range but have very modest performance (see the inset of Fig. 5b), especially for their equiatomic compositions (solid symbols). These $|\Delta S_{isothermal}^{peak}|$ values mainly saturate to less than 1 J kg^{-1} K^{-1} over a wide $T_{transition}$ range in the chart, while the non-equiatomic RE-free HEAs enable at least an order of magnitude enhancement (represented as the open circles and dash lines in Fig. 5b) [22, 23]. However, it has to be noted that such magnitudes are still not competitive to high-performing conventional magnetocaloric materials due to the distributed exchange interactions that occur from the disorder as pointed out in refs. [24, 25]. Despite this, extending beyond the equiatomic HEA region has indeed enlarged the compositional space of HEAs, where it lies a wide window of opportunities in obtaining appropriate compositions with good magnetocaloric properties. The key to finding the solution to this challenge of locating large MCE in the huge compositional space is to perform an effective search in this large region with the targeted goal in mind. This has been recently reported in refs. [26, 27] where a significant improvement in the MCE is found for RE-free HEAs, whose data are plotted as the greenish open circles and dash lines in Fig. 5b. The literature data collected for plotting Fig. 5 are further tabulated in Tables 1 and 2 for RE-containing and RE-free magnetocaloric HEAs, respectively (Ref. [11] provides a supplementary document with the various MCE parameters).

TABLE 1: Literature data collected for the performance comparison of equiatomic vs. non-equiatomic RE-containing amorphous magnetocaloric HEAs for 5 T.

RE-containing amorphous Magnetocaloric HEAs		$T_{transition}$ (K)	$\left\lvert \Delta S_{isothermal}^{peak} \right\rvert$ (J kg^{-1} K^{-1}) 5 T	Ref.
Equiatomic	TmHoErCoAl	9	15.00	[28]
	TmDyErCoAl	13	11.9	[29]
	TmHoErCoCu	13.5	15.73	[30]
	DyHoErCoAl	18	12.60	[28]
	GdTbDyHoErYNiCoAgAl	24	10.64	[31]
	GdHoErNiAl	25	9.50	[14]
	TbDyErCoAl	29	8.60	[29]
	GdHoTmNiCu	32	10.60	[32]
	GdTmErCoAl	32.1	9.70	[33]
	GdHoErCoAl bulk	37	11.20	[28]
	GdHoErCoAl wires	39	10.20	[14]
	GdYCoAl	39	6.02	[34]
	Gd$_{25}$(Y$_{0.6}$Ho$_{0.4}$)$_{25}$Co$_{25}$Al$_{25}$	41	7.35	[34]
	GdDyErCoAl	43	9.10	[29]
	Gd$_{25}$(Y$_{0.6}$Er$_{0.4}$)$_{25}$Co$_{25}$Al$_{25}$	43	6.96	[34]
	Gd$_{25}$(Y$_{0.4}$Dy$_{0.4}$)$_{25}$Co$_{25}$Al$_{25}$	44	6.76	[34]
	GdTbDyAlNi	45	7.25	[35]
	Gd$_{25}$(Y$_{0.4}$Ho$_{0.6}$)$_{25}$Co$_{25}$Al$_{25}$	47	7.61	[36]
	GdHoErCoCu	49	11.10	[15]
	Gd$_{25}$(Y$_{0.2}$Ho$_{0.8}$)$_{25}$Co$_{25}$Al$_{25}$	49	8.79	[36]
	GdHoCoAl	50	9.78	[37]
	GdHoErNiCo	50	6.52	[38]
	Gd$_{25}$(Y$_{0.04}$Ho$_{0.96}$)$_{25}$Co$_{25}$Al$_{25}$	51	8.63	[36]
	GdHoErFeAl	55	5.10	[14]
	GdTbDyAlCo	58	9.43	[35]
	GdDyCoAl	60	8.72	[37]
	GdTbCoAl	73	8.88	[37]
	GdTbDyAlFe	112	5.96	[35]
Non-equiatomic	Gd$_{18}$Ho$_{22}$Tm$_{20}$Cu$_{22}$Al$_{18}$	33.6	8.70	[39]
	Gd$_{36}$Tb$_{20}$Co$_{20}$Al$_{24}$	81	8.90	[21]
	(Gd$_{36}$Tb$_{20}$Co$_{20}$Al$_{24}$)$_{99}$Fe$_1$	94	8.50	[21]
	Gd$_{19}$Tb$_{19}$Er$_{18}$Fe$_{19}$Al$_{25}$	97	5.90	[40]
	(Gd$_{36}$Tb$_{20}$Co$_{20}$Al$_{24}$)$_{98}$Fe$_2$	100	8.00	[21]
	(Gd$_{36}$Tb$_{20}$Co$_{20}$Al$_{24}$)$_{97}$Fe$_3$	108	7.60	[21]

The comparison case discussed in the text is highlighted in bold

A game changer in magnetocaloric HEAs

As the MCE is intrinsic to magnetic materials, it is very common to find researchers designing for large magnetization values in magnetocaloric materials, which is also the case for magnetocaloric HEAs. Thus, their compositional designs center on using ferromagnetic TM elements (such as Fe, Co, Ni, etc.) as well as RE elements (due to their large intrinsic magnetic moments). However, combining such elements, especially in large concentrations to design for multicomponent alloys in HEAs, be it all RE-HEAs or HEAs with combination of RE and ferromagnetic TM elements, most likely leads to a compensated magnitude in the overall magnetization value of the alloy. This could be due to the average performance from the various elements or to the coupling effects among the elements. Hence, the typical magnetocaloric HEAs often shows sub-par performance as well as a broadened MCE, especially for those shown in the abovementioned sections.

Although extending the compositional space for HEAs from equiatomic to non-equiatomic does alleviate magnetocaloric HEA limitations by increasing the opportunity window, this large degree of freedom in HEA search resembles of finding a needle in the haystack. It is challenging to perform search in the vast HEA space in a rational and efficient manner although there are many high-throughput tools developed today for predictions or synthesis experiments. They will need an appropriate starting

TABLE 2: Literature data collected for the performance comparison of equiatomic vs. non-equiatomic RE-free magnetocaloric HEAs for 2 T.

RE-free Magnetocaloric HEAs		$T_{transition}$ (K)	$\left\lvert \Delta S_{isothermal}^{peak} \right\rvert$ (J kg^{-1} K^{-1}) 2 T	Ref.
Equiatomic	Annealed $Fe_{24.1}Co_{24.1}Ni_{24.1}Cr_{27.7}$	36	0.38	[41]
	As-rolled $Fe_{24.1}Co_{24.1}Ni_{24.1}Cr_{27.7}$	43	0.34	[41]
	Annealed $Fe_{24.39}Co_{24.39}Ni_{24.39}Cr_{26.83}$	48	0.37	[41]
	As-rolled $Fe_{24.39}Co_{24.39}Ni_{24.39}Cr_{26.83}$	59	0.34	[41]
	Annealed $Fe_{24.69}Co_{24.69}Ni_{24.69}Cr_{25.93}$	65	0.36	[41]
	As-rolled $Fe_{24.69}Co_{24.69}Ni_{24.69}Cr_{25.93}$	71	0.34	[41]
	As-rolled $FeCoNiCr$	100	0.35	[41]
	As-rolled $Fe_{25.3}Co_{25.3}Ni_{25.3}Cr_{24.1}$	131	0.35	[41]
	Annealed $Fe_{25.64}Co_{25.64}Ni_{25.64}Cr_{23.08}$	148	0.38	[41]
	$FeCoNi_{1.5}Cr_{0.5}Al$	150	0.28	[42]
	As-rolled $Fe_{25.64}Co_{25.64}Ni_{25.64}Cr_{23.08}$	171	0.35	[41]
	As-rolled $Fe_{26}Co_{26}Ni_{26}Cr_{22}$	193	0.37	[41]
	Annealed $Fe_{23.53}Co_{23.53}Ni_{23.53}Cr_{23.53}Pd_{5.88}$	210	0.40	[12]
	$FeCoNiCr$	270	0.56	[12]
	$FeCoNi_{0.5}Cr_{0.5}$	270	0.56	[43]
	$FeCoNiCrAl$	290	0.23	[42]
	$AlCrFeCoNiCu$ thin films	295	0.18	[44]
	$FeCoNi_{0.5}Cr_{0.5}Al_{1.5}$	455	0.50	[43]
	$Fe_{25}Co_{25}Ni_{25}(Mo_{0.2}P_{0.4}B_{0.4})_{25}$	560	1.00	[45]
	$FeCoNi_{0.5}Cr_{0.5}Al$	685	0.40	[43]
Non-equiatomic	$Fe_{26.7}Ni_{26.7}Mn_{20}Ga_{15.6}Si_{11}$	334	1.59	[23]
	$Mn_{24}Cr_{10}Ni_{33}Ge_{25}Si_{8}$	387	3.6	[46]
	$Mn_{27}Cr_{7}Ni_{33}Ge_{25}Si_{8}$	412	2.49	[22]
	$Mn_{22.3}Fe_{22.2}Ni_{22.2}Ge_{16.65}Si_{16.65}$ **(FOPT)**	143	5.33	[26]
	$Mn_{22.3}Fe_{22.2}Ni_{22.2}Ge_{15.82}Si_{17.48}$ **(FOPT)**	181	5.80	[27]
	$Mn_{22.3}Fe_{22.2}Ni_{22.2}Ge_{14.95}Si_{18.35}$ **(FOPT)**	203	10.21	[27]

The large enhancement in MCE found for FOPT are highlighted in bold

composition to maximize the full potential of these advanced techniques.

Another method of improving MCE is to consider the fact that its large magnitude lies near the transition temperature, where an abrupt dM/dT in Eq. 1 (also presented in Fig. 2) will lead to a large MCE. Materials that show the most abrupt change are those which undergo first-order phase transitions (FOPT). The earlier-mentioned HEAs exhibit gradual dM/dT, undergoing second-order phase transitions (SOPT). Hence, the hypothesis for large MCE enhancement in HEAs is the existence of FOPT in the vast HEA space. This has been recently reported by Law et al., by using a targeted property search strategy in the HEA space for further performance optimization, achieving significant MCE values ($\left\lvert \Delta S_{isothermal}^{peak} \right\rvert = 13.1$ J kg^{-1} K^{-1} for 2.5 T) in RE-free HEAs [27].

Targeted property search strategy

A comparison of the earlier-mentioned HEA design schemes versus the targeted property search strategy is presented as schematic ternary phase diagrams (for simplicity) in Fig. 6. The conventional alloys based on one or two constituents followed by dilution of minor additions are found at the corners of the phase diagram. The yellow center of the phase diagram indicates the equiatomic HEA composition. Thus, Fig. 6a indicates the first design strategy adopted for designing magnetocaloric HEAs, which is to increase the number of principal elements with equiatomic compositions. The magnetocaloric HEA design approach evolves from equiatomic to non-equiatomic compositions as depicted in Fig. 6b. It has to be highlighted that the extension endeavors have been made with equiatomic compositions as the starting point as indicated by the arrows. In this case, the challenge is to determine for the search direction that will lead to the desired property. Contrastingly, the targeted property search strategy that helps us find large MCE values in RE-free HEAs reverses the direction of the search arrows as shown in Fig. 6c. The starting composition is selected from conventional alloys already with the desired behavior intended, which exhibits a FOPT, and tuned it toward the HEA space, in combination with the following considerations:
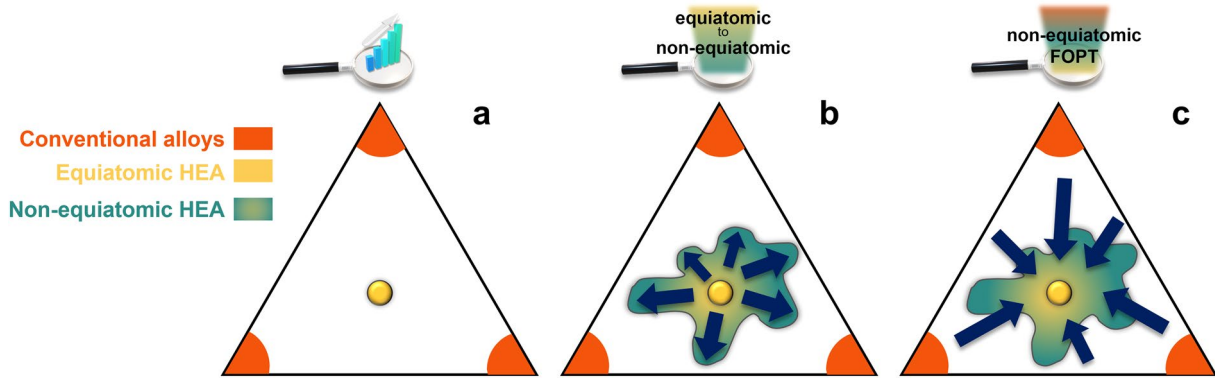
Figure 6: The various approaches taken for designing magnetocaloric HEAs: (a) increasing number of principal elements, (b) extending from equiatomic to non-equiatomic HEA compositions and (c) targeted property search strategy.

(i) choosing doping element(s) with chemically compatibility for isostructural substitutions, and.

(ii) preserving the elemental stoichiometry (including the substitutions).

The Fe–Mn-Ni-Ge-Si HEA case

One of the cases where magnetocaloric materials undergo a FOPT and give a large MCE is associated with the presence of a magnetostructural transformation. With this aim, Law et al. tuned FOPT-MnNiSi toward HEA region with isostructural substitutions of Fe and Ge in appropriate concentrations, resulting
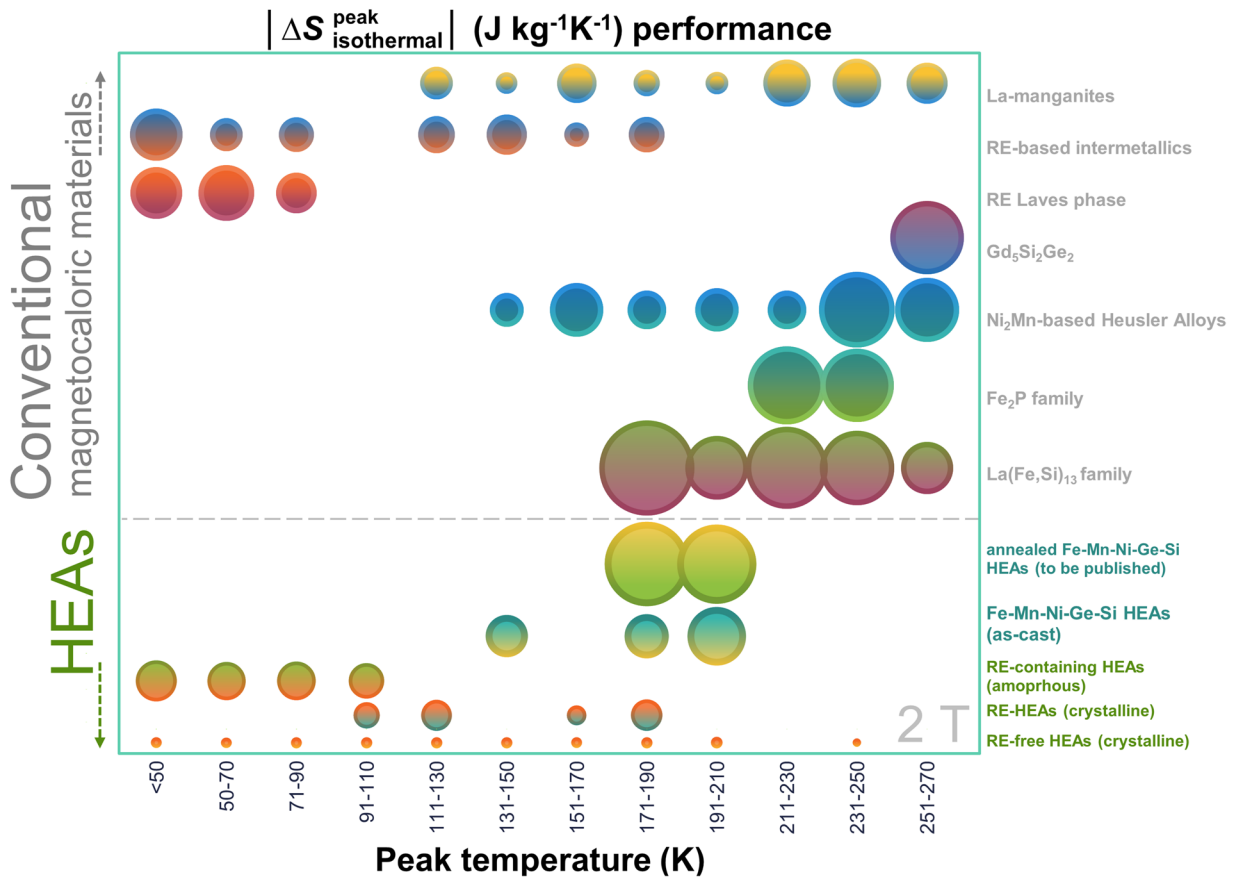

Figure 7: Magnetocaloric performance matrix for magnetocaloric HEAs (greenish text labels) vs high-performance conventional magnetocaloric materials (gray text labels) for 2 T. The gray dash line in the matrix is a guide to the eye for separating these two groups of samples. Size of the circles corresponds to $\left| \Delta S_{\text{isothermal}}^{\text{peak}} \right|$. Literature data collected from refs. [4, 12, 16, 18, 19, 21, 26–28, 36, 47–53].

in a magnetostructural transformation in RE-free quinary $Fe_{22.2}Mn_{22.3}Ni_{22.2}Ge_{16.65}Si_{16.65}$ ($\Delta S_{mix} = 1.60$ R) as evidenced in their thermomagnetic data and temperature-dependent synchrotron X-ray diffraction results [26].

Further performance optimization was made by varying the Ge/Si ratio following this starting composition in $Fe_{22.2}Mn_{22.3}Ni_{22.2}Ge_xSi_y$ HEAs, while adhering to the second condition of the directed search approach [27]. Their magnetostructural transformation temperatures are further tuned to higher temperatures (from 143 to 203 K) in addition to an ~79% increase in $\left|\Delta S_{isothermal}^{peak}\right|$ (refer to Ref. [27] for more details). This MCE enhancement not only finds Fe–Mn–Ni–Ge–Si HEAs with the largest magnitude of $\left|\Delta S_{isothermal}^{peak}\right|$ among magnetocaloric HEAs, but it also closes the pre-existing gap of magnetocaloric HEAs versus high-performing conventional magnetocaloric materials. This is depicted in the performance matrix presented in Fig. 7 where the sizes of the circles represent the magnitude of $\left|\Delta S_{isothermal}^{peak}\right|$ with a dashed line separating the two groups of materials: conventional versus HEAs. In addition, annealing of Fe–Mn–Ni–Ge–Si HEAs further optimize their performance,

specified temperature span and has been widely used as an alternate figure of merit of magnetocaloric materials for avoiding the artificially large refrigerant capacity of shallow peaks. As HEAs comprise of multiple principal elements in large concentrations, they typically show very broad MCE due to the dilution of the overall magnetization of the alloy. Although reports frequently highlight for their large refrigerant capacity values, this could be misleading unless the peak entropy change is also large, which is usually not the case. Thus, the *TEC* figure of merit plays an essential role in evaluating for the performance of magnetocaloric HEAs. It is calculated using the following equation:

$$TEC(\Delta T_{lift}) = \frac{1}{\Delta T_{lift}} \max_{T_{mid}} \int_{T_{mid}-\frac{1}{2}\Delta T_{lift}}^{T_{mid}+\frac{1}{2}\Delta T_{lift}} \Delta S(T)_{\Delta H,T} dT, (3)$$

where ΔT_{lift} represents the specified range of temperatures (usually 3–10 K) and T_{mid} refers to the temperature corresponding to the center of the average. In cases that the whole magnetocaloric curve is not available, such as analyzing work from literature reports, a *TEC* approximation has been found in good agreement with calculated values [21]. This simplification of calculating for $TEC(\Delta T_{lift})$ is approximated as:

$$TEC(\Delta T_{lift}) \approx \frac{\Delta S_{isothermal}(T_{peak}-\frac{1}{2}\Delta T_{lift}) + \Delta S_{isothermal}(T_{peak}) + \Delta S_{isothermal}(T_{peak}+\frac{1}{2}\Delta T_{lift})}{3} \quad (4)$$

as recently presented by the same co-authors in conferences, finding MCE magnitudes that are as competitive as the highly regarded conventional materials, La(Fe,Si)$_{13}$ and Fe$_2$P [47].

Methods of MCE analysis applicable to HEA systems

Being magnetocalorics an emergent topic for HEAs, many of their reports focus on studying the microstructural, phase transition temperatures and the $\Delta S_{isothermal}$ of magnetocaloric HEAs. Due to many of their reports on MCE broadening behavior, in this section, we only select the appropriate developed tools among all others used for further analyzing magnetocaloric materials. They include the temperature averaged entropy change (*TEC*) and universal scaling. More recently, the MCE field dependence exponent *n* has been used for revealing the multiphases in magnetocaloric HEAs as well as for evaluating if the new alloys undergo a FOPT or SOPT.

Temperature averaged entropy change

The temperature averaged entropy change, $TEC(\Delta T_{lift})$ [54], relates to the maximum average of the $\Delta S_{isothermal}$ over a

where T_{peak} is the temperature corresponding to $\left|\Delta S_{isothermal}^{peak}\right|$.

Universal curves method

Scaling laws [55] have been widely applied to magnetocaloric materials, especially to evaluate for the order of phase transitions they undergo and to extrapolate MCE values at higher or lower magnetic fields for literature comparison. This method is based on the assumption that a SOPT scales. Thus, when the rescaled magnetocaloric curves collapse onto a universal curve, it indicates that it is a SOPT magnetocaloric material, which is also successfully applicable to the adiabatic temperature change [56].

Rescaling of $\Delta S_{isothermal}(T)$ curves measured for different maximum magnetic fields is performed by following a phenomenological procedure [57]:

(i) Normalizing the $\Delta S_{isothermal}(T)$ curves to their respective $\left|\Delta S_{isothermal}^{peak}\right|$ values (they are field dependent),
(ii) Rescaling the temperature axis with reference temperature (T_r) by imposing that the reference points in the curve correspond to $\theta = \pm 1$, where

$$\theta = (T - T_C)/(T_r - T_C) \quad (5)$$

and T_r is selected at the corresponding points where 0.5 – 0.7 times of $\left|\Delta S_{\text{isothermal}}^{\text{peak}}\right|$. These rescaled curves (plots of normalized $\Delta S_{\text{isothermal}}$ versus θ) have all their normalized $\Delta S_{\text{isothermal}}$ data fall at the same θ point, being then said to collapse onto a universal curve, when the scaling laws are applicable to the material.

Universal scaling had been applied to families of Finemet, Nanoperm, HiTperm, and bulk amorphous alloys [58], which are soft magnetic amorphous alloys with SOPT character. The rescaled curves collapse onto a single universal curve, further confirming the order of the transition. Subsequently, the types of materials tested were significantly extended to rare-earths, crystalline phases, etc. [55].

It has to be noted that when the results do not collapse onto a single universal curve, it can imply that there are several magnetic phases with their SOPTs overlapping one another [59] or that the demagnetizing field of the samples is not negligible [60]. These effects could be resolved by rescaling the temperature axis with two T_r:

$$\theta = \begin{cases} -(T - T_C)/(T_{r,1} - T_C), & T \le T_C \\ (T - T_C)/(T_{r,2} - T_C), & T > T_C \end{cases} \quad (6)$$

where T_{r1} and T_{r2} are selected at the corresponding points where 0.5 – 0.7 times of $\left|\Delta S_{\text{isothermal}}^{\text{peak}}\right|$ below and above T_c.

In addition, this universal scaling analysis can further uncover the presence of additional thermomagnetic phase transitions [61], indicating for a multiphase composite even when a single MCE peak is apparently observed. In the case of composites, deviations from the universal curve become more apparent when phase fractions or the MCE responses of the several coexisting phases are similar (for further details on magnetocaloric composite materials, readers can refer to ref. [5]). Recently, a phase deconvolution procedure based on universal scaling of the MCE has been successfully applied to a biphasic SOPTs composite for predicting the response of the pure constituent phases [62] and then further extended to deconvolute SOPT from FOPT in a Heuser alloy [63]. Refs. [3, 55] summarize further applications of the universal curves procedure. There have been many magnetocaloric HEA reports that include the universal scaling method to show that their new alloys undergo SOPT. However, as these new HEAs are frequently multiphase materials, we expect an increase of the publications applying the abovementioned phase deconvolution procedures to identify the response of each of the individual phases. In this way, it would be possible to determine to what extent additional synthesis efforts for obtaining a phase-pure alloy of a specific composition would enhance the performance of the material.

When the universal curve cannot be obtained even by using Eq. (6) and the sample is single phase, this can be used as a qualitative method that overcomes the contradiction between experimental calorimetric data of FOPT material and results from Banerjee´s criterion [64] as reported in ref. [65].

MCE field dependence exponent *n*

As the order of phase transition plays a main role in the magnitude of MCE, it is particularly important to determine the order of phase transitions in magnetocaloric materials, including magnetocaloric HEAs. Many authors rely on the quantitative Banerjee´s criterion [64], which identifies SOPT when the Arrott plots ((H/M) as a function of M^2) show positive slopes and FOPT when there are negative slopes. Since the earlier-mentioned discrepancies with calorimetric data of FOPT magnetocaloric material (as reported in ref. [65]), an alternate quantitative criterion based on the MCE has been developed by Law et al. [66]. This new method is based on the magnetic field dependence of $\Delta S_{\text{isothermal}}$ expressed as: $\Delta S_{\text{isothermal}} \propto H^n$, where exponent *n* is field and temperature dependent, as illustrated in Fig. 8. It can be locally calculated as:

$$n = \frac{\text{d}\ln|\Delta S_{\text{isothermal}}|}{\text{d}\ln H} \quad (7)$$

The fingerprint for FOPT identifies an overshoot of $n > 2$ near the transition temperature and its absence indicates for a SOPT. It has to be taken into account that in cases of a direct MCE switching into an inverse MCE, the *n* features will indicate for the characteristic switching signs instead of a FOPT. As an example, a schematic illustration of the MCE types, FOPT criterion (in yellowish shade) and the sign-switching features (pattern-filled) is presented. Figure 8(a) shows the direct MCE undergoing FOPT and SOPT and their exponent *n* in Fig. 8(b) yields an overshoot of $n > 2$ near the transition temperature for FOPT. For a sample exhibiting both inverse and direct MCE as shown in Fig. 8(c), its FOPT exponent *n* criterion (Fig. 8(d)) is observed near the transition temperature of inverse MCE while the sign-switching characteristic feature should be noted in the pattern-filled region. In the reports of the FOPT magnetocaloric HEAs, this exponent *n* criterion was applied for identifying the FOPT [26, 27].

In addition, exponent *n* as a function of temperature has been used for identifying the presence of multiphases in Gd–Tb–Co–Al–Fe HEAs [21, 67]. The authors found broadened widths in the minima of $n(T)$ curves for their samples, which attribute to the observed enhancement in the refrigerant capacity values.
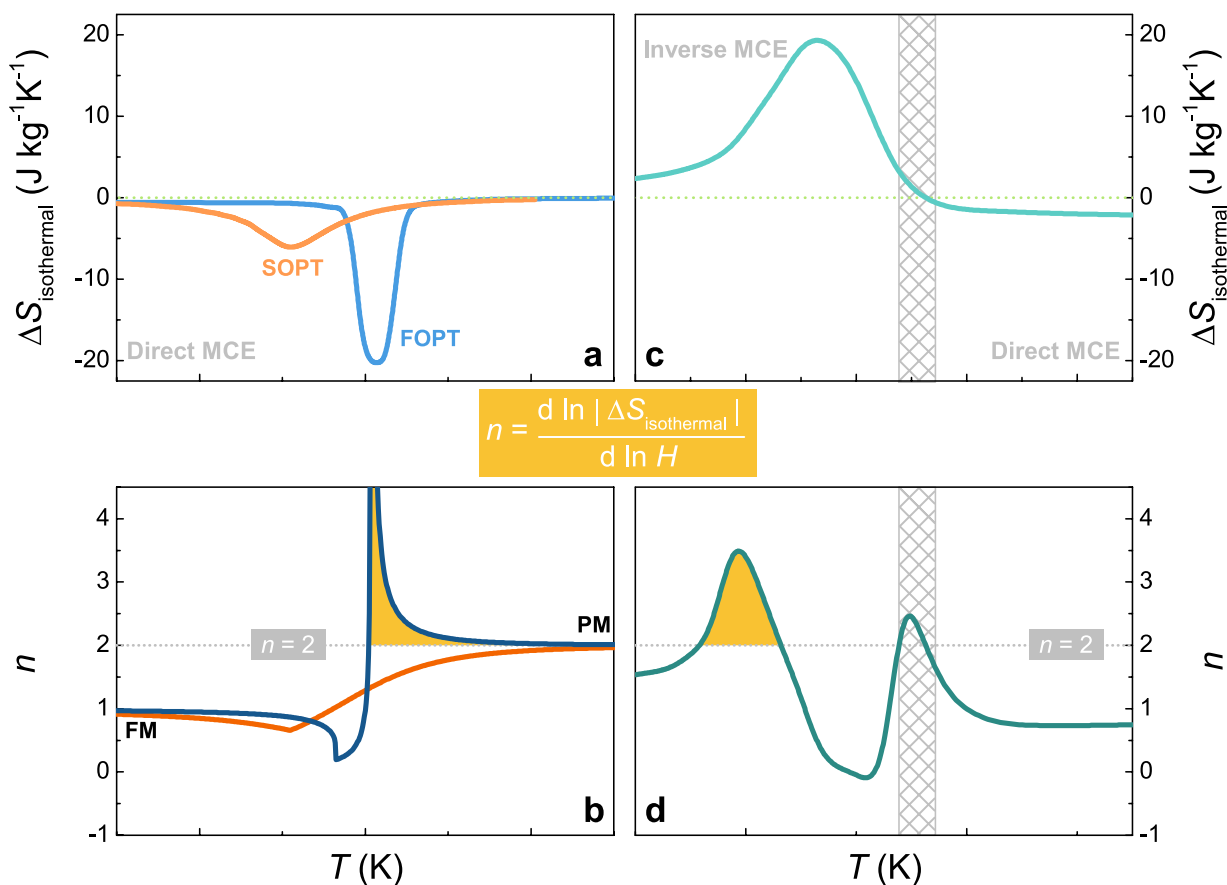
$$n = \frac{d \ln |\Delta S_{isothermal}|}{d \ln H}$$

Figure 8: Schematic representation of the (a) direct MCE and (b) its exponent n as a function of temperature. In panel (c), a sample showing both inverse and direct MCE is schematically illustrated with its exponent n presented in (d). The overshoot of $n > 2$ criterion for FOPT (shaded in yellowish color) is observed for cases of ferromagnetic (FM) → paramagnetic (PM) in panel (a) as well as from inverse MCE as shown in panel (c). Characteristic features of switching the signs of isothermal entropy change (pattern-filled region) in (d) should not be mistaken as the FOPT criterion.

Temperature first-order reversal curve (TFORC)

In spite of a significantly larger magnetocaloric response, FOPTs come at a cost, namely the presence of thermal hysteresis, which is undesirable for magnetocaloric refrigeration. Recently, an extension of the first-order reversal curve analysis (FORC) to thermal hysteresis, called TFORC [68], has been developed. It can provide valuable information on the origin of hysteresis and fine details about the transformation kinetics that occurs in the material. In particular, the combination of modeling [69] and experimentation with well-known samples [70], allows the identification of unexpected processes that take place in the samples under study.

For performing these TFORC experiments, the temperature of the sample has to be increased to the point of complete transformation (saturation) then it must be swept back to a certain reversal temperature in the hysteretic region. Starting from that reversal temperature, the measurement of $M(T)$ back to saturation is called first-order reversal curve. This procedure is repeated for a complete set of reversal temperatures and, by performing the cross-derivative of magnetization

vs. temperature and reversal temperature, the distribution of individual square hysteresis loops that conforms the full process is obtained. This TFORC distribution would present characteristic features that can be identified from a catalogue, providing valuable knowledge about the processes that the material undergoes [3].

While TFORC has been studied on different magnetocaloric materials, it has not yet been studied on HEAs. The reason for this absence of studies is that until very recently, MCE-HEAs did not exhibit a FOPT, making TFORC unapplicable. Considering that HEAs with large MCE are now associated with FOPT, we anticipate a surge of these studies.

Outlook

The HEA design concept yields newly unexplored compositional space in multicomponent alloy phase diagrams that could provide breakthroughs in structural and defense applications via combinations of properties. Thus, this propels the interest in advancing the design idea to functional sectors, which can

directly address the current limitations of functional materials. This is especially so for the limited mechanical stability faced by conventional magnetocaloric materials with high-performance for magnetic refrigeration.

While the efforts of exploring HEAs for magnetocalorics are surging, only the recent breakthrough with a targeted search strategy into the HEA compositional space found magnetocaloric properties that show HEAs´ potential for this functional application. The implementation of magnetostructural behavior in HEAs greatly boosts their MCE performance to be on-par with conventional high-performing magnetocaloric materials. While this design method has led to some clear and quantifiable parameters for designing competitive magnetocaloric HEA compositions, exploration and development of HEAs with high MCE performance along these lines will be required as the field evolves. Efficient property optimization can be then enabled with the help of high-throughput predictive thermodynamic models, and/or compositional substitutions and processing techniques. There are precedents of shape memory alloys exhibiting martensitic transformation that can have good mechanical integrity upon cycling as well as superplasticity. Therefore, the objective of discovering HEAs with first-order magnetostructural phase transition accompanied by mechanical integrity should be reachable.

With the know-how approach to designing competent magnetocaloric HEAs, combining them with optimal mechanical properties and economic viability, reliability of devices would be improved and service life would be extended. Thus, this leads to improving sustainability in various sectors. This spurs the search for competitive magnetocaloric HEAs, which is still at an ascent stage. Clear pathways of designing such HEAs and understanding their material and property analysis play important roles in this development.

Funding

Data availability

Data available on request from the authors.

Declarations

Conflict of interest Authors declare no conflict of interests.

Ethical approval

Not applicable.

Open Access

References

1. Enerdata, Enerdata - Global Energy Trends 2021 Edition. *World Energy & Climate Statistics* www.enerdata.et (2021).

2. TMS: Defining Pathways for Realizing the Revolutionary Potential of High Entropy Alloys (TMS, 2021).

3. V. Franco, Á. Díaz-García, L.M. Moreno-Ramirez, J.Y. Law, Magnetocaloric characterization for the study of phase transitions, in *Magnetic Cooling: From Fundamentals to High Efficiency Refrigeration*. ed. by K.G. Sandeman, O. Gutfleisch (Wiley, New York, 2023)

4. V. Franco, J.S. Blazquez, J.J. Ipus, J.Y. Law, L.M. Moreno-Ramirez, A. Conde, Magnetocaloric effect: from materials research to refrigeration devices. Prog Mater Sci. **93**, 112 (2018)

5. J.Y. Law and V. Franco: Magnetocaloric Composite materials, in Encyclopedia of Materials: Composites, ed. by D. Brabazon (Elsevier, New York, 2021), pp. 461.

6. A. Kitanovski, Energy Applications of Magnetocaloric Materials. Adv. Energy Mater. **10**(10), 1903741 (2020)

7. A. Kitanovski, J. Tušek, U. Tomc, U. Plaznik, M. Ožbolt, A. Poredoš, *Magnetocaloric Energy Conversion: From Theory to Applications* (Springer, Cham, 2015)

8. D.B. Miracle, O.N. Senkov, A critical review of high entropy alloys and related concepts. Acta Mater. **122**, 448 (2017)

9. M.C. Gao, J.-W. Yeh, P.K. Liaw, Y. Zhang, *High Entropy Alloys: Fundamentals and Applications* (Springer, New York, 2016)

10. J.-W. Yeh, S.-K. Chen, S.-J. Lin, J.-Y. Gan, T.-S. Chin, T.-T. Shun, C.-H. Tsau, S.-Y. Chang, Nanostructured high-entropy alloys with multiple principal elements: novel alloy design concepts and outcomes. Adv. Eng. Mater. **6**(5), 299 (2004)

11. J.Y. Law, V. Franco, Pushing the limits of magnetocaloric high-entropy alloys. APL Mater. **9**(8), 080702 (2021)

12. D.D. Belyea, M.S. Lucas, E. Michel, J. Horwath, C.W. Miller, Tunable magnetocaloric effect in transition metal alloys. Sci Rep. **5**, 15755 (2015)

13. Z. Dong, S. Huang, V. Ström, G. Chai, L.K. Varga, O. Eriksson, L. Vitos, $MnxCr_{0.3}Fe_{0.5}Co_{0.2}Ni_{0.5}Al_{0.3}$ high entropy alloys for magnetocaloric refrigeration near room temperature. J Mater Sci Technol. **79**, 15 (2021)

14. W. Sheng, J.-Q. Wang, G. Wang, J. Huo, X. Wang, R.-W. Li, Amorphous microwires of high entropy alloys with large magnetocaloric effect. Intermetallics **96**, 79 (2018)

15. L. Li, C. Xu, Y. Yuan, S. Zhou, Large refrigerant capacity induced by table-like magnetocaloric effect in amorphous $Er_{0.2}Gd_{0.2}Ho_{0.2}Co_{0.2}Cu_{0.2}$ ribbons. Mater. Res. Lett. **6**(8), 413 (2018)

16. Y. Yuan, Y. Wu, X. Tong, H. Zhang, H. Wang, X.J. Liu, L. Ma, H.L. Suo, Z.P. Lu, Rare-earth high-entropy alloys with giant magnetocaloric effect. Acta Mater. **125**, 481 (2017)

17. H. Yin, Effect of microstructure on magnetocaloric properties of high entropy alloys, Double PhD from Harbin University of Technology (China) and University of Seville (Spain) (2022)

18. S.F. Lu, L. Ma, G.H. Rao, J. Wang, Y.S. Du, L. Li, J.T. Zhao, X.C. Zhong, Z.W. Liu, Magnetocaloric effect of high-entropy rare-earth alloy GdTbHoErY. J. Mater. Sci. **32**, 10919 (2021)

19. S.F. Lu, L. Ma, J. Wang, Y.S. Du, L. Li, J.T. Zhao, G.H. Rao, Effect of configuration entropy on magnetocaloric effect of rare earth high-entropy alloy. J. Alloys Compd. **874**, 159918 (2021)

20. Z. Li, K.G. Pradeep, Y. Deng, D. Raabe, C.C. Tasan, Metastable high-entropy dual-phase alloys overcome the strength–ductility trade-off. Nature **534**, 227 (2016)

21. H. Yin, J. Law, Y. Huang, V. Franco, H. Shen, S. Jiang, Y. Bao, J. Sun, Design of Fe-containing GdTbCoAl high-entropy-metallic-glass composite microwires with tunable Curie temperatures and enhanced cooling efficiency. Mater. Des. **206**, 109824 (2021)

22. K. Sarlar, A. Tekgül, I. Kucuk, Magnetocaloric properties in a FeNiGaMnSi high entropy alloy. Curr Appl Phys. **20**(1), 18 (2020)

23. K. Sarlar, A. Tekgul, I. Kucuk, Magnetocaloric properties of rare-earth-free $Mn_{27}Cr_7Ni_{33}Ge_{25}Si_8$ high-entropy alloy. IEEE Magn. Lett. **10**, 2109905 (2019)

24. A. Perrin, M. Sorescu, V. Ravi, D.E. Laughlin, M.E. McHenry, Mössbauer analysis of compositional tuning of magnetic exchange interactions in high entropy alloys. AIP Adv. **9**(3), 035329 (2019)

25. A. Perrin, D.E. Laughlin, M.E. McHenry, *High Entropy Alloys: Magnetocaloric Effects, in Encyclopedia of Materials: Metals and Alloys* (Elsevier, New York, 2021)

26. J.Y. Law, L.M. Moreno-Ramírez, Á. Díaz-García, A. Martín-Cid, S. Kobayashi, S. Kawaguchi, T. Nakamura, V. Franco, MnFeNiGeSi high-entropy alloy with large magnetocaloric effect. J. Alloys Compd. **855**, 157424 (2021)

27. J.Y. Law, Á. Díaz-García, L.M. Moreno-Ramírez, V. Franco, Increased magnetocaloric response of FeMnNiGeSi high-entropy alloys. Acta Mater. **212**, 116931 (2021)

28. J. Huo, L. Huo, J. Li, H. Men, X. Wang, A. Inoue, C. Chang, J.-Q. Wang, R.-W. Li, High-entropy bulk metallic glasses as promising magnetic refrigerants. J. Appl. Phys. **117**(7), 073902 (2015)

29. J. Li, L. Xue, W. Yang, C. Yuan, J. Huo, B. Shen, Distinct spin glass behavior and excellent magnetocaloric effect in $Er_{20}Dy_{20}Co_{20}Al_{20}RE_{20}$ (RE = Gd, Tb and Tm) high-entropy bulk metallic glasses. Intermetallics **96**, 90 (2018)

30. Z. Dong, Z. Wang, S. Yin, Magnetic properties and large cryogenic magneto-caloric effect of $Er_{0.2}Tm_{0.2}Ho_{0.2}Cu_{0.2}Co_{0.2}$ amorphous ribbon. Intermetallics **124**, 106879 (2020)

31. J. Huo, J.-Q. Wang, W.-H. Wang, Denary high entropy metallic glass with large magnetocaloric effect. J. Alloys Compd. **776**, 202 (2019)

32. Y. Zhang, B. Wu, D. Guo, J. Wang, Z. Ren, Magnetic properties and promising cryogenic magneto-caloric performances of $Gd_{20}Ho_{20}Tm_{20}Cu_{20}Ni_{20}$ amorphous ribbons. Chin. Phys B. **30**(1), 017501 (2021)

33. M. Cai, Q. Luo, Q. Zeng, B. Shen, Combined effect of demagnetization field and magnetic anisotropy on magnetocaloric behavior and magnetocaloric-magnetoresistance correlation in GdTmErCoAl high-entropy amorphous alloy. J Magn Magn Mater. **528**, 167817 (2021)

34. C.M. Pang, L. Chen, H. Xu, W. Guo, Z.W. Lv, J.T. Huo, M.J. Cai, B.L. Shen, X.L. Wang, C.C. Yuan, Effect of Dy, Ho, and Er substitution on the magnetocaloric properties of Gd-Co-Al-Y high entropy bulk metallic glasses. J. Alloys Compd. **827**, 154101 (2020)

35. J. Huo, L. Huo, H. Men, X. Wang, A. Inoue, J. Wang, C. Chang, R.-W. Li, The magnetocaloric effect of Gd-Tb-Dy-Al-M (M = Fe, Co and Ni) high-entropy bulk metallic glasses. Intermetallics **58**, 31 (2015)

36. C.M. Pang, C.C. Yuan, L. Chen, H. Xu, K. Guo, J.C. He, Y. Li, M.S. Wei, X.M. Wang, J.T. Huo, B.L. Shen, Effect of Yttrium addition on magnetocaloric properties of Gd-Co-Al-Ho high entropy metallic glasses. J. Non-Cryst. Solids **549**, 120354 (2020)

37. L. Xue, L. Shao, Q. Luo, B. Shen, $Gd_{25}RE_{25}Co_{25}Al_{25}$ (RE = Tb, Dy and Ho) high-entropy glassy alloys with distinct spin-glass behavior and good magnetocaloric effect. J. Alloys Compd. **790**, 633 (2019)

38. Y. Zhang, J. Zhu, S. Li, J. Wang, Z. Ren, Achievement of giant cryogenic refrigerant capacity in quinary rare-earths based high-entropy amorphous alloy. J. Mater. Sci. Technol. **102**, 66 (2022)

39. Z. Dong, Z. Wang, S. Yin, Magnetic properties and magneto-caloric effect (MCE) in $Cu_{22}Al_{18}Ho_{22}Tm_{20}Gd_{18}$ amorphous ribbons. J. Magn. Magn. Mater. **514**, 167270 (2020)

40. L. Luo, H. Shen, Y. Bao, H. Yin, S. Jiang, Y. Huang, S. Guo, S. Gao, D. Xing, Z. Li, J. Sun, Magnetocaloric effect of melt-extracted high-entropy $Gd_{19}Tb_{19}Er_{18}Fe_{19}Al_{25}$ amorphous microwires. J. Magn. Magn. Mater. **507**, 166856 (2020)

41. M.S. Lucas, D. Belyea, C. Bauer, N. Bryant, E. Michel, Z. Turgut, S.O. Leontsev, J. Horwath, S.L. Semiatin, M.E. McHenry, C.W. Miller, Thermomagnetic analysis of $FeCoCr_xNi$ alloys: Magnetic entropy of high-entropy alloys. J. Appl. Phys. **113**(17), 17A923 (2013)

42. S.-M. Na, P.K. Lambert, H. Kim, J. Paglione, N.J. Jones, Thermomagnetic properties and magnetocaloric effect of FeCoNiCrAl-type high-entropy alloys. AIP Adv. **9**(3), 035010 (2019)

43. A. Quintana-Nedelcos, Z. Leong, N.A. Morley, Study of dual-phase functionalisation of $NiCoFeCr-Al_x$ multicomponent alloys for the enhancement of magnetic properties and magneto-caloric effect. Mater. Today Energy. **20**, 100621 (2021)

44. S. Vorobiov, O. Pylypenko, Y. Bereznyak, I. Pazukha, E. Čižmár, M. Orendáč, V. Komanicky, Magnetic properties, magnetoresistive, and magnetocaloric effects of AlCrFeCoNiCu thin-film high-entropy alloys prepared by the co-evaporation technique. Appl. Phys. A **127**(3), 179 (2021)

45. K. Wu, C. Liu, Q. Li, J. Huo, M. Li, C. Chang, Y. Sun, Magnetocaloric effect of $Fe_{25}Co_{25}Ni_{25}Mo_5P_{10}B_{10}$ high-entropy bulk metallic glass. J. Magn. Magn. Mater. **489**, 165404 (2019)

46. A. Tekgül, K. Sarlar, N. Küçük, A.B. Etemoglu, The structural, magnetic and magnetocaloric properties of MnCrNiGeSi high-entropy alloy. Phys. Scr. **97**, 075814 (2022)

47. Á. Díaz-García, J.Y. Law, L.M. Moreno-Ramirez, R. Schäfer and V. Franco: To be published (2022)

48. Y. Zhang, Review of the structural, magnetic and magnetocaloric properties in ternary rare earth RE_2T_2X type intermetallic compounds. J. Alloys Compd. **787**, 1173 (2019)

49. T.L. Phan, T.A. Ho, T.V. Manh, N.T. Dang, C.U. Jung, B.W. Lee, T.D. Thanh, Y-doped $La_{0.7}Ca_{0.3}MnO_3$ manganites exhibiting a large magnetocaloric effect and the crossover of first-order and second-order phase transitions. J. Appl. Phys. **118**(14), 143902 (2015)

50. L.M. Moreno-Ramírez, C. Romero-Muñiz, J.Y. Law, V. Franco, A. Conde, I.A. Radulov, F. Maccari, K.P. Skokov, O. Gutfleisch, Tunable first order transition in La(Fe, Cr, $S_i)13$ compounds: retaining magnetocaloric response despite a magnetic moment reduction. Acta Mater. **175**, 406 (2019)

51. L.M. Moreno-Ramírez, C. Romero-Muñiz, J.Y. Law, V. Franco, A. Conde, I.A. Radulov, F. Maccari, K.P. Skokov, O. Gutfleisch, The role of Ni in modifying the order of the phase transition of La(Fe, Ni, $S_i)13$. Acta Mater. **160**, 137 (2018)

52. B. Kaeswurm, V. Franco, K.P. Skokov, O. Gutfleisch, Assessment of the magnetocaloric effect in La, Pr(Fe, Si) under cycling. J. Magn. Magn. Mater. **406**, 259 (2016)

53. J.Y. Law, Á. Díaz-García, L.M. Moreno-Ramírez, V. Franco, A. Conde, A.K. Giri, How concurrent thermomagnetic transitions can affect magnetocaloric effect: the $Ni_{49-x}Mn_{36+x}In_{15}$ Heusler alloy case. Acta Mater. **166**, 459 (2019)

54. J.Y. Fan, B. Hong, D. Lu, Y.G. Shi, L.S. Ling, L. Zhang, W. Tong, L. Pi, Y.H. Zhang, Magnetocaloric effect of half-doped manganite $Nd_{0.5}Ca_{0.25}Sr_{0.25}MnO_3$. Physica B **405**(15), 3120 (2010)

55. V. Franco, A. Conde, Scaling laws for the magnetocaloric effect in second order phase transitions: from physics to applications for the characterization of materials. Int. J. Refrig. **33**(3), 465 (2010)

56. V. Franco, A. Conde, J.M. Romero-Enrique, Y.I. Spichkin, V.I. Zverev, A.M. Tishin, Field dependence of the adiabatic temperature change in second order phase transition materials: application to Gd. J. Appl. Phys. **106**(10), 103911 (2009)

57. V. Franco, J.S. Blazquez, A. Conde, Field dependence of the magnetocaloric effect in materials with a second order phase transition: a master curve for the magnetic entropy change. Appl. Phys. Lett. **89**(22), 222512 (2006)

58. V. Franco, J.S. Blazquez, M. Millan, J.M. Borrego, C.F. Conde, A. Conde, The magnetocaloric effect in soft magnetic amorphous alloys. J. Appl. Phys. **101**(9), 09C503 (2007)

59. V. Franco, R. Caballero-Flores, A. Conde, Q.Y. Dong, H.W. Zhang, The influence of a minority magnetic phase on the field dependence of the magnetocaloric effect. J. Magn. Magn. Mater. **321**(9), 1115 (2009)

60. C. Romero-Muñiz, J.J. Ipus, J.S. Blazquez, V. Franco, A. Conde, Influence of the demagnetizing factor on the magnetocaloric effect: critical scaling and numerical simulations. Appl. Phys. Lett. **104**(25), 252405 (2014)

61. V. Franco, A. Conde, V.K. Pecharsky, K.A. Gschneidner, Field dependence of the magnetocaloric effect in Gd and ($Er_{1-x}Dy_x$) Al_2: does a universal curve exist? Epl-Europhys Lett. **79**(4), 47009 (2007)

62. Á. Díaz-García, J.Y. Law, P. Gębara, V. Franco, Phase deconvolution of multiphasic materials by the universal scaling of the magnetocaloric effect. JOM **72**(8), 2845 (2020)

63. Á. Díaz-García, J.Y. Law, L.M. Moreno-Ramírez, A.K. Giri, V. Franco, Deconvolution of overlapping first and second order phase transitions in a NiMnIn Heusler alloy using the scaling laws of the magnetocaloric effect. J. Alloys Compd. **871**, 159621 (2021)

64. B.K. Banerjee, On a generalised approach to first and second order magnetic transitions. Phys. Lett. **12**(1), 16 (1964)

65. C.M. Bonilla, J. Herrero-Albillos, F. Bartolome, L.M. Garcia, M. Parra-Borderias, V. Franco, Universal behavior for magnetic entropy change in magnetocaloric materials: an analysis on the nature of phase transitions. Phys Rev B. **81**(22), 224424 (2010)

66. J.Y. Law, V. Franco, L.M. Moreno-Ramirez, A. Conde, D.Y. Karpenkov, I. Radulov, K.P. Skokov, O. Gutfleisch, A quantitative

criterion for determining the order of magnetic phase transitions using the magnetocaloric effect. Nat. Commun. **9**(1), 2680 (2018)

67. H. Yin, J.Y. Law, Y. Huang, H. Shen, S. Jiang, S. Guo, V. Franco, J. Sun, Enhancing the magnetocaloric response of high-entropy metallic-glass by microstructural control. Sci. China Mater. **65**(4), 1134 (2022)

68. V. Franco, T. Gottschall, K.P. Skokov, O. Gutfleisch, First-order reversal curve (FORC) analysis of magnetocaloric Heusler-type alloys. IEEE Magn. Lett. **7**, 6602904 (2016)

69. L.M. Moreno-Ramírez, V. Franco, Setting the basis for the interpretation of temperature first order reversal curve (TFORC) distributions of magnetocaloric materials. Metals **10**(8), 1039 (2020)

70. Á. Díaz-García, L.M. Moreno-Ramírez, J.Y. Law, F. Albertini, S. Frabbrici, V. Franco, Characterization of thermal hysteresis in magnetocaloric NiMnIn Heusler alloys by temperature first order reversal curves (TFORC). J. Alloys Compd. **867**, 159184 (2021)